

The radial distribution of galactic gamma rays

II. The distribution of cosmic-ray electrons and nuclei in the outer Galaxy

J. B. G. M. Bloemen^{1, **}, K. Bennett⁶, G. F. Bignami², L. Blitz^{*, **}, P. A. Caraveo², M. Gottwald^{4, ***}, W. Hermsen¹, F. Lebrun⁵, H. A. Mayer-Hasselwander⁴, and A. W. Strong²

The Caravane Collaboration for the COS-B satellite

¹ Laboratory for Space Research Leiden, Leiden, The Netherlands

² Istituto di Fisica Cosmica del CNR, Milano, Italy

³ Istituto di Fisica Cosmica e Informatica del CNR, Palermo, Italy

⁴ Max-Planck-Institut für Physik und Astrophysik, Institut für Extraterrestrische Physik, D-8046 Garching bei München, Federal Republic of Germany

⁵ Service d'Astrophysique, Centre d'Etudes Nucléaires de Saclay, F-91191 Gif-sur-Yvette, France

⁶ Space Science Department of the European Space Agency, ESTEC, Noordwijk, The Netherlands

Received August 29, 1983; accepted January 16, 1984

Summary. The radial distribution of the high-energy (70 MeV–5 GeV) gamma-ray emissivity in the outer Milky Way is derived. The kinematics of H I are used to construct column-density maps in various galacto-centric distance ranges in the outer Galaxy. These maps are used in combination with COS-B gamma-ray data to determine gamma-ray emissivities in these distance ranges. A steep negative gradient of the emissivity for the 70 MeV–150 MeV energy range is found in the outer Galaxy. The emissivity for the 300 MeV–5 GeV range is found to be approximately constant (within $\sim 20\%$) and equal to the local value out to large (~ 20 kpc) galacto-centric distances. These results imply a hardening of the gamma-ray spectrum with increasing distance. For $R > 16$ kpc the spectrum is shown to be significantly different from the local gamma-ray spectrum and consistent with a π^0 -decay spectrum having the intensity expected from the local measurement of the cosmic-ray nuclei spectrum. Results obtained from a similar but more limited analysis of the SAS-2 data are in agreement with the COS-B findings. The energy-dependent decrease is interpreted as a steep gradient in the cosmic-ray electron density and a near constancy of the nuclear component. The variation of the electron component is shown to be consistent with low-frequency radio continuum observations. The galactic origin of electrons with energies up to several hundreds of MeV is confirmed, while for cosmic-ray nuclei with energies of a few GeV either confinement in a large galactic halo or an extragalactic origin is suggested by the data.

Key words: cosmic rays – gamma rays – interstellar matter – COS-B

Send offprint requests to: J.B.G.M. Bloemen, Huygens Laboratorium, Wassenaarseweg 78, NL-2300 RA Leiden, The Netherlands

* Astronomy program, University of Maryland, USA

** Also Sterrewacht, Huygens Laboratorium, Leiden, The Netherlands

*** Present address: ESOC, D-6100 Darmstadt, Federal Republic of Germany

I. Introduction

The diffuse component of galactic high-energy (≥ 35 MeV) gamma rays has long been interpreted to be mainly the result of the interaction of cosmic-ray electrons (via bremsstrahlung) and cosmic-ray nuclei (via π^0 decay) with the interstellar gas (e.g. Stecker, 1971). To date these two contributions have not been separated observationally despite their different spectral shapes. Lebrun et al. (1982) and Strong et al. (1982) using COS-B data, and Strong and Wolfendale (1981), Thompson and Fichtel (1982), and Lebrun and Paul (1983) using SAS-2 data, have shown that locally ($\lesssim 1$ kpc) a good correlation exists between the gamma-ray intensity and the total gas column density at medium latitudes. Various authors have shown that in the galactic plane the major part of the gamma-ray emission can be explained by cosmic-ray interactions with the gas as traced by H I and ^{12}CO observations [see e.g. Arnaud et al. (1982) and Lebrun et al. (1983)].

For the outer Galaxy, Bloemen et al. (1984; Paper I) analysing COS-B data, have shown that the gamma-ray intensity (150 MeV–5 GeV, 70 MeV–5 GeV) is proportional to the H I column density alone (i.e. H_2 can be neglected) within the uncertainties of the analysis. From the radial distribution of the H I, with which the gamma rays are correlated, they conclude that a significant fraction of the galactic gamma-ray emission originates at large galacto-centric distances and that $\sim 50\%$ of the total gamma-ray luminosity of the Galaxy is produced beyond the solar circle.

The gamma-ray emissivity for the 70 MeV–5 GeV energy range derived in Paper I is $\sim 15\%$ lower than the local value determined by Strong et al. (1982). This decrease, if statistically significant, is mainly due to a reduced emissivity ($\sim 30\%$) of the low-energy (70 MeV–150 MeV) component. Both, from the SAS-2 data (Dodds et al., 1975; Issa et al., 1980, 1981; Wolfendale, 1981) and from the COS-B data (Mayer-Hasselwander et al., 1982), previous indications were found for a lower gamma-ray emissivity in the outer Galaxy compared to the local value.

In this paper the relatively good counting statistics of the COS-B experiment are exploited to determine the gamma-ray emissivities for the second and third galactic quadrants in various galacto-centric distance ranges and three energy intervals. A similar analysis is performed on the SAS-2 data. Using the COS-B

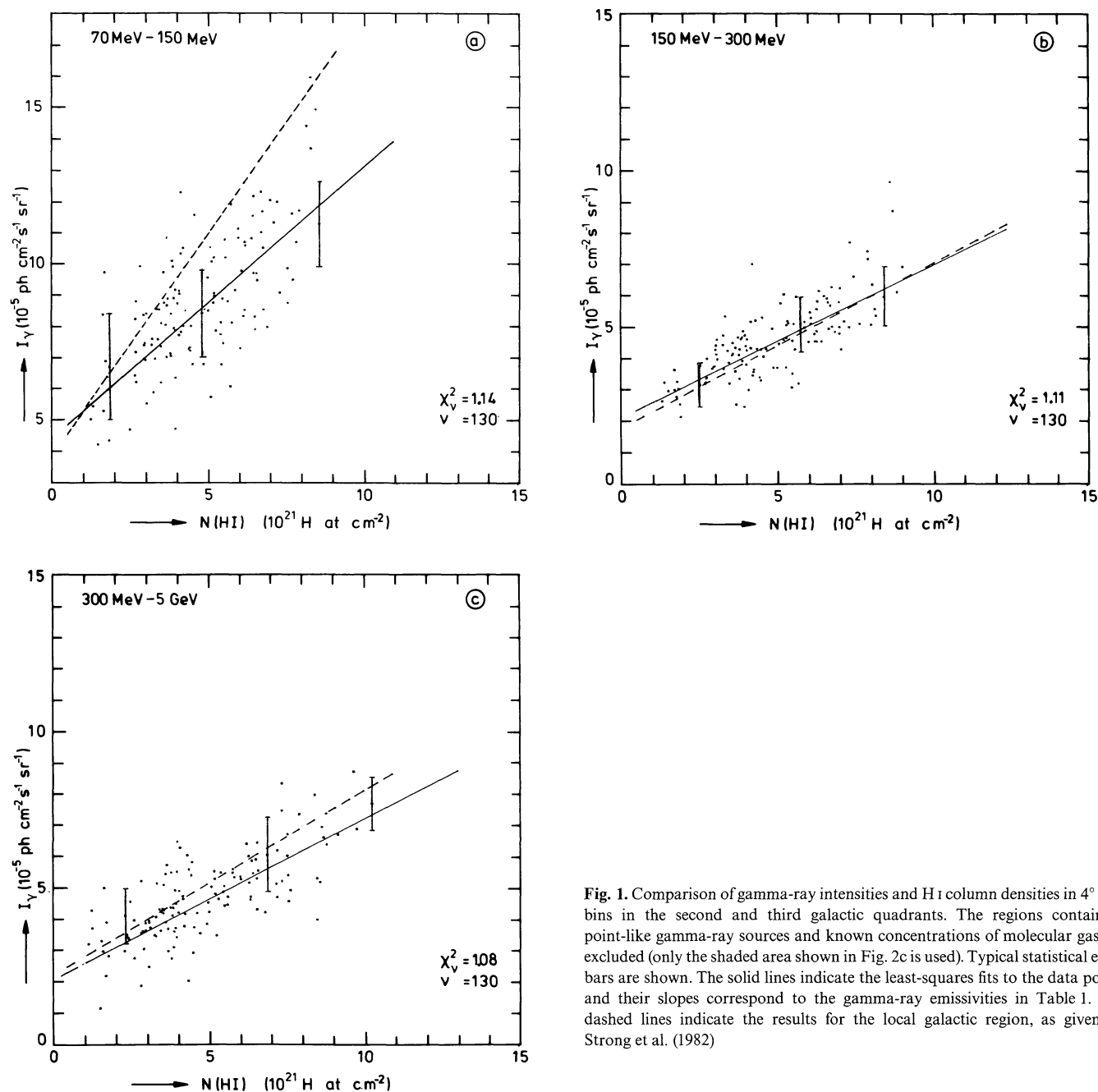


Fig. 1. Comparison of gamma-ray intensities and HI column densities in $4^\circ \times 4^\circ$ bins in the second and third galactic quadrants. The regions containing point-like gamma-ray sources and known concentrations of molecular gas are excluded (only the shaded area shown in Fig. 2c is used). Typical statistical error bars are shown. The solid lines indicate the least-squares fits to the data points and their slopes correspond to the gamma-ray emissivities in Table 1. The dashed lines indicate the results for the local galactic region, as given by Strong et al. (1982)

data, the gamma-ray emissivity spectrum is derived for three distance ranges and is discussed in terms of the contribution from bremsstrahlung and π^0 decay and of the distribution of cosmic rays. Finally, the observed low-frequency synchrotron emission is compared with the prediction based on the derived radial distribution of cosmic-ray electrons. Some implications for the origin of cosmic-ray nuclei are discussed.

II. Gamma-ray emissivities in the outer Galaxy

Since the molecular hydrogen can be neglected for $R > R_\odot$ (in this paper we take $R_\odot = 10$ kpc) the 21-cm line surveys alone, together with the gamma-ray surveys, can be used to determine gamma-ray

emissivities in the outer Galaxy. Regions with known concentrations of molecular gas were excluded.

a) The average emissivities

The gamma-ray emissivities averaged over the total line-of-sight in the second and third galactic quadrants can be determined by a comparison of the total HI column densities with the gamma-ray intensities I_γ . This analysis was performed in Paper I for the energy ranges 70 MeV–5 GeV and 150 MeV–5 GeV and has been repeated here for three independent energy intervals (70 MeV–150 MeV, 150 MeV–300 MeV and 300 MeV–5 GeV) to investigate the energy dependence of the decrease of the gamma-ray emissivity compared to the local value.

Table 1. Average gamma-ray emissivities q_γ in the second and third galactic quadrants ($|b| < 10^\circ$), as determined from the comparison of I_γ in three energy ranges with $N(\text{H I})$. I_b represents the total isotropic (mainly instrumental) background. Statistical 1σ errors are given. The local emissivities (and corresponding I_b values) are those given by Strong et al. (1982)

E	Outer Galaxy		Locally	
	$q_\gamma/4\pi$ 10^{-26} photon H atom $^{-1}$ s^{-1} sterad $^{-1}$	I_b 10^{-5} photon cm^{-2} s^{-1} sterad $^{-1}$	$q_\gamma/4\pi$ 10^{-26} photon H atom $^{-1}$ s^{-1} sterad $^{-1}$	I_b 10^{-5} photon cm^{-2} s^{-1} sterad $^{-1}$
70 MeV–150 MeV	0.87 ± 0.07	4.3 ± 0.7	(a) 1.4	(b) 3.9
150 MeV–300 MeV	0.49 ± 0.04	2.1 ± 0.3	0.53	1.7
300 MeV– 5 GeV	0.50 ± 0.04	2.0 ± 0.3	0.59	2.3

(a) These values have statistical uncertainties of about 10% (see discussion in Bloemen et al., 1984)

(b) Strong et al. give residual values relative to estimated isotropic backgrounds of 4.6, 1.7, and 1.9 in the three energy ranges, respectively

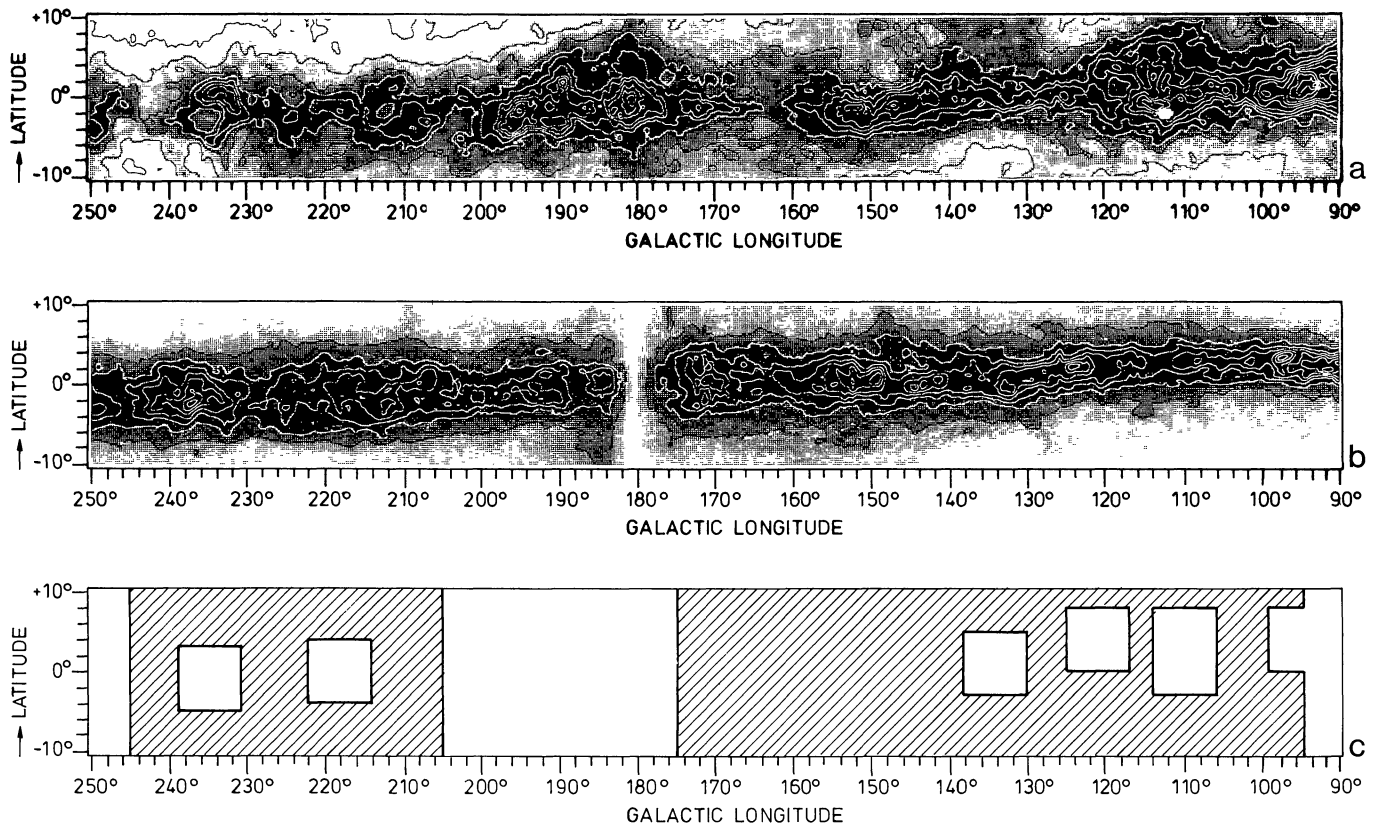


Fig. 2a–c. H I column-density maps for $R < 15$ kpc (a) and $R > 15$ kpc (b). Contour values: (1, 2, 3, ...) 10^{21} H atom cm^{-2} . The shaded area shown in c indicates the region used in the present analysis

The analysis was performed in the longitude range covered by the H I surveys of Weaver and Williams (1973) and Heiles and Habing (1974) in the second and third galactic quadrants. Those regions where contamination from pointlike gamma-ray sources (Swanenburg et al., 1981) and known concentrations of molecules between $l \cong 107^\circ$ and $l \cong 113^\circ$ might affect the analysis were excluded (*a posteriori* it was verified that inclusion of these regions, except for the regions containing the two strong gamma-ray sources in the anti centre, would not have changed the conclusions

reached in this paper). The remaining data were analyzed in the longitude range $95^\circ < l < 245^\circ$ and the latitude range $|b| < 10^\circ$. The H I surveys were corrected to obtain the brightness temperature T_b (Williams, 1973), and a first order optical-depth correction was made assuming an uniform spin temperature of 125 K. A column-density map was constructed and convolved with the COS-B point-spread functions (Hermsen, 1980) for the energy ranges to be analyzed. Gamma-ray intensity maps in the three energy ranges were derived from the COS-B data base described

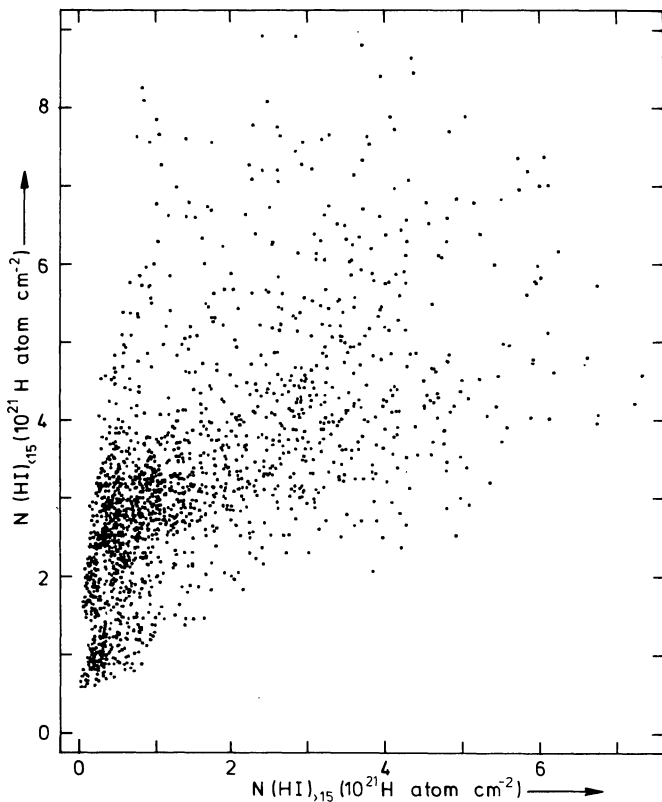


Fig. 3. Comparison of H I column densities for $R < 15$ kpc and $R > 15$ kpc in $1^\circ \times 1^\circ$ bins in the second and third galactic quadrants. The regions containing point-like gamma-ray sources and known concentrations of molecular gas are excluded (only the shaded area shown in Fig. 2c is used)

by Mayer-Hasselwander et al. (1982), supplemented by later observations. The derivation of gamma-ray intensities requires knowledge of the measured gamma-ray spectrum in order to take into account the energy dependence of the instrument response. An E^{-2} spectrum as derived for the diffuse emission in the solar neighbourhood (e.g. Lebrun et al., 1982) was assumed. The impact of this assumption on the results was evaluated *a posteriori* and, where significant, the results have been corrected.

The data were analyzed by fitting I_γ and $N(\text{H I})$ in $4^\circ \times 4^\circ$ bins for the three energy ranges, using a relation of the form

$I_\gamma = \frac{1}{4\pi} q_\gamma \tilde{N}(\text{H I}) + I_b$, where $\tilde{N}(\text{H I})$ is the convolved H I column density. The results are presented in Fig. 1a–c. The slope of the least-squares fit defines the gamma-ray emissivity q_γ in the three energy ranges, the values of which are given in Table 1. The level of the isotropic background (mainly instrumental) was left as a free parameter to be defined by the offset of the fit, as given in Table 1. Table 1 also includes the local emissivity values and background levels determined by Strong et al. (1982) using COS-B data at medium galactic latitudes. The background levels determined from the present analysis are in good agreement with the values determined by Strong et al. For the 150 MeV–300 MeV and 300 MeV–5 GeV energy ranges q_γ is equal to the local value within the uncertainties. For the low-energy range (70 MeV–150 MeV), however, q_γ is $\sim 60\%$ of the local value. The decrease is larger than the systematic uncertainty quoted by Strong et al. in determining the local emissivity values. Therefore we proceeded to determine

the distribution of q_γ as a function of galacto-centric radius for the three energy ranges.

b) The radial distribution of emissivities

The velocity information available from the 21-cm line can be used to determine the spatial distribution of the H I for $R > R_\odot$. We used the rotation curve of the outer Galaxy given by Blitz et al. (1980) as modified by Kulkarni et al. (1982) to determine distances beyond the solar circle. Using this distance information, H I column densities can be determined in various galacto-centric distance ranges and their contribution to the observed gamma-ray intensities can be investigated.

To illustrate the sensitivity of the method, we determined first the average gamma-ray emissivities in only two distance ranges, namely: $10 \text{ kpc} < R < 15 \text{ kpc}$ and $R > 15 \text{ kpc}$. The analysis was performed over the same region of the second and third galactic quadrants and on the same H I and gamma-ray data as described in Sect. IIa. H I column-density maps have been constructed for the gas in the two distance intervals (see Fig. 2a and b) and have been convolved with the COS-B point-spread functions as in Sect. IIa.

The distributions of $N(\text{H I})$ in both distance ranges are quite different. On a large scale this is due to the warp of the hydrogen layer, which is more pronounced for $R > 15 \text{ kpc}$ [see e.g. Henderson et al. (1982) and Kulkarni et al. (1982)]. Although the scale height of the H I layer increases for increasing galacto-centric distances, the distribution of the H I column densities outside 15 kpc shows a relatively narrow latitude extent compared to the wider distribution of the column densities inside 15 kpc. On smaller scales, the clumpiness of the atomic hydrogen distribution produces distinct differences between the distributions of $N(\text{H I})$ in the two distance ranges. These differences in the projected distributions allow the following two-dimensional correlation analysis. Figure 2c presents the area which remains after the exclusion of the regions containing the point-like gamma-ray sources and well known concentrations of molecular gas. For this remaining region we show in Fig. 3 pictorially that the structures in the distribution of $N(\text{H I})$ for the two distance ranges are significantly different. Presented are comparisons between column densities of H I inside 15 kpc and outside 15 kpc in $1^\circ \times 1^\circ$ bins. It is clear from this scatter diagram that the quantities exhibit a large degree of independence.

We investigated which combination of gamma-ray emissivities inside 15 kpc ($q_{\gamma, <15}$) and outside 15 kpc ($q_{\gamma, >15}$) best describes the observed gamma-ray distribution, using a relation of the form:

$$I_\gamma = \frac{1}{4\pi} q_{\gamma, <15} \tilde{N}(\text{H I})_{<15} + \frac{1}{4\pi} q_{\gamma, >15} \tilde{N}(\text{H I})_{>15} + I_b, \quad (1)$$

where $\tilde{N}(\text{H I})_{<15}$ and $\tilde{N}(\text{H I})_{>15}$ are the convolved H I column densities. I_b represents the total isotropic background. A maximum-likelihood method, similar to that used by Lebrun et al. (1982), was applied on $1^\circ \times 1^\circ$ bins to determine $q_{\gamma, <15}$, $q_{\gamma, >15}$ and I_b for each energy range. Using the likelihood ratio λ , defined as the ratio of the likelihood L maximized over I_b and the likelihood maximized over all three parameters (L^*), $\lambda(q_{\gamma, <15}, q_{\gamma, >15}) = \left(\frac{\max L}{L^*} \right)$, a confidence region can be assigned to $q_{\gamma, <15}$ and $q_{\gamma, >15}$, knowing that $-2\text{Ln}\lambda$ has a chi-square distribution with 2 degrees of freedom (Eadie et al., 1971). Figure 4d–f show the confidence contours of the emissivities for the three energy ranges. The analysis was also performed for two additional distance cuts R_c : for $R < 12.5 \text{ kpc}$ and $R > 12.5 \text{ kpc}$ and for

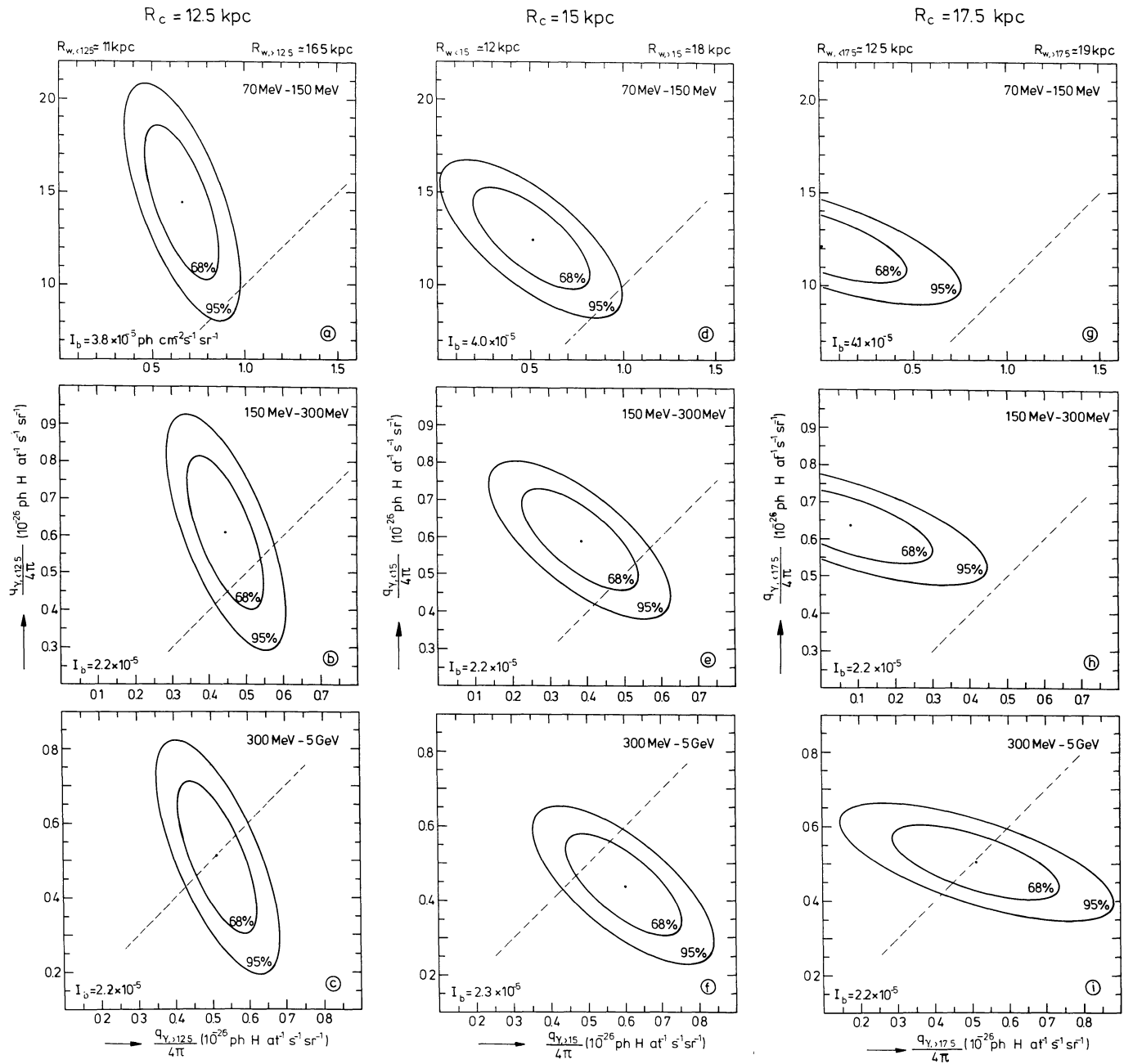


Fig. 4a-i. Likelihood contours of $q_{\gamma, <R_c}$ and $q_{\gamma, >R_c}$ for three energy ranges. The distributions are shown for $R_c = 12.5$ kpc (a-c), $R_c = 15$ kpc (d-f) and $R_c = 17.5$ kpc (g-i). The dashed lines indicate $q_{\gamma, <R_c} = q_{\gamma, >R_c}$. The 68% and 95% confidence levels indicated, are determined from the distribution of the likelihood ratio λ (see Sect. IIb). Assuming that the quantity $-2\ln\lambda$ has a chi-square distribution with 2 degrees of freedom, the corresponding values of $-2\ln\lambda$ are 2.4 and 6.0, respectively. The maximum-likelihood estimates of the isotropic-background parameter I_b are given in each figure. For each distance interval, the weighted galactocentric distance R_w [determined iteratively from the average radial distribution of $N(H I)$ and the resulting emissivity distribution] is indicated

$R < 17.5$ kpc and $R > 17.5$ kpc. The resulting confidence regions of the emissivities are also presented in Fig. 4. The maximum-likelihood estimates of I_b are given in each figure and are again consistent with the values determined by Strong et al. (1982).

As the axes of the ellipses are not parallel to the coordinate axes, the derived values of $q_{\gamma, <R_c}$ and $q_{\gamma, >R_c}$ (with R_c equals 12.5 kpc, 15 kpc and 17.5 kpc) are not completely independent, which is primarily due to some degree of correlation between the maps of $\tilde{N}(H I)_{<R_c}$ and $\tilde{N}(H I)_{>R_c}$. However, the confidence regions

show a clear energy dependent difference between the values of $q_{\gamma, <R_c}$ and $q_{\gamma, >R_c}$. Namely, for all three distance cuts there is a trend indicating that $q_{\gamma, >R_c}$ is smaller than $q_{\gamma, <R_c}$ for the 70 MeV–150 MeV range (with an average confidence probability of $\sim 95\%$), while no significant differences are present for the two higher-energy ranges. This allows the conclusion that the gamma-ray emissivity for low-energy (70–150 MeV) gamma rays shows a stronger decrease outside the solar circle than the emissivity for higher-energy (150 MeV–5 GeV) gamma rays. In fact, for the 300 MeV–5 GeV range, the emissivity remains

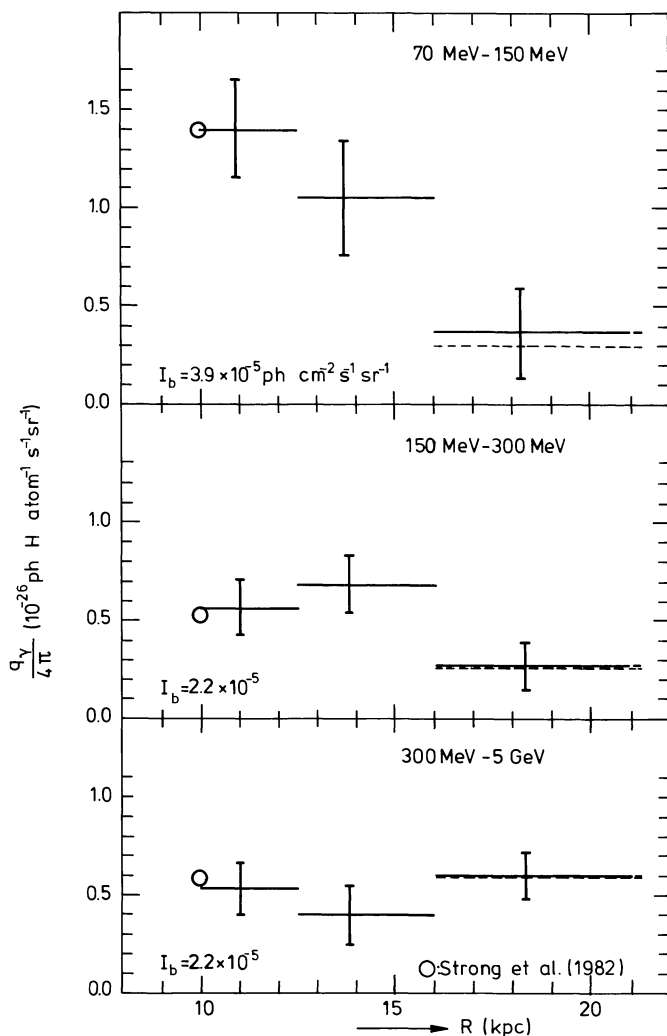


Fig. 5. Radial distribution of q_γ in the outer Galaxy for three energy ranges. Formal errors (1σ) are indicated. The resulting isotropic background values I_b are given in the figures. The local emissivity values determined by Strong et al. (1982) are indicated for $R=10$ kpc. These values have statistical uncertainties of about 10% (see discussion in Bloemen et al. 1984). The dashed lines for $R > 16$ kpc show the values of q_γ after correction for a π^0 -decay input spectrum (see Sect. III)

approximately constant out to large (~ 20 kpc) galactocentric distances.

Since the average H I column density outside 15 kpc is $\sim 30\%$ of the total average column density in the second and third galactic quadrants ($|b| < 10^\circ$), it is clear from these emissivities that gamma-ray emission related to gas outside 15 kpc contributes significantly to the observed high-energy gamma-ray intensity, as shown in Paper I.

The various emissivity values shown in Fig. 4 suggest a smooth R dependence of the emissivity. However, because the distance ranges overlap, the derived emissivities are not independent. To obtain an independent set of values as a function of R , we determined q_γ in three distinct distance intervals: $R < 12.5$ kpc, 12.5 kpc $< R < 16$ kpc and $R > 16$ kpc. The distance intervals were chosen so that comparable fractions of the total average H I column density are contained in each interval. H I column-density maps were constructed for these ranges and the analysis was

repeated, using a relation of the same form as Eq. (1), but in this case with three H I terms. The resulting values of these 4-parameter fits are presented in Fig. 5. Formal errors (1σ) were determined from the distribution of the maximum-likelihood ratios (Eadie et al., 1971). The decrease in emissivity for the 70 MeV–150 MeV energy range as a function of galactocentric radius and the near constancy (within 20%) for high energies (300 MeV–5 GeV), is evident from this figure. The local emissivities determined by Strong et al. (1982) are included in Fig. 5 for $R=10$ kpc and they fit the trend present in each energy range.

c) Complementary analysis of the SAS-2 data

From analyses of SAS-2 data it has been claimed that for energies above 100 MeV (Dodds et al., 1975) and for the 35 MeV–100 MeV energy range (Issa et al., 1980), the emissivities in the outer Galaxy are lower than the local values. However, conclusions on the energy dependence of the decrease of the gamma-ray emissivity cannot be drawn from their differing analyses. In performing their analysis for both ranges Wolfendale (1981) and Issa et al. (1981) found, for $R \lesssim 14$ kpc, “some slight evidence” for a stronger decrease in the low-energy range. We therefore wish to verify whether our analysis when applied to the SAS-2 data, also gives an energy dependence of the emissivities. The digitized SAS-2 data base in these energy ranges (Fichtel et al., 1978) has been analyzed here for the second and third galactic quadrants in a comparable way to that described for the COS-B data in Sect. IIb.

The intensity scales of the COS-B and SAS-2 experiments were normalized in the region $60^\circ > l > 300^\circ$ and $|b| < 10^\circ$, assuming an E^{-2} input spectrum as described in detail by Strong et al. (1984). This action was taken to avoid systematic differences in the results due to uncertainties in the absolute calibration and the differences in the input spectra assumed to calculate the sensitive areas. The region containing two strong gamma-ray sources (Crab and 2CG 195+04), has been excluded from the analysis. The analysis was performed only for the distance ranges $R < 15$ kpc and $R > 15$ kpc.

Since the counting statistics of the SAS-2 experiment are relatively poor, a 3-parameter fit ($q_{\gamma, < 15}$, $q_{\gamma, > 15}$ and I_b) could not satisfactorily determine I_b . Therefore the isotropic background component I_b was fixed to the value determined by comparing the gamma-ray intensities with total column-density estimates from galaxy counts at medium latitudes (Thompson and Fichtel, 1982; Lebrun and Paul, 1983), adopting the galaxy-counts calibration of Strong and Lebrun (1982). These values are $I_b \cong 6 \cdot 10^{-5}$ photon $\text{cm}^{-2} \text{s}^{-1} \text{sterad}^{-1}$ for the 35–100 MeV range and $I_b \cong 2 \cdot 10^{-5}$ photon $\text{cm}^{-2} \text{s}^{-1} \text{sterad}^{-1}$ for energies above 100 MeV (see Strong et al., 1984).

Figure 6 shows the confidence contours of the emissivities for both energy ranges. Again, the axes of the ellipses are not parallel to the coordinate axes, indicating that $q_{\gamma, < 15}$ and $q_{\gamma, > 15}$ are not completely independent. However, the confidence levels allow the conclusion that the gamma-ray emissivity for low-energy gamma rays (35–100 MeV) decreases significantly faster outside the solar circle than the emissivity for the high-energy (> 100 MeV) range, in agreement with the hint for a gradient found by Issa et al. (1981) and Wolfendale (1981) for $R \lesssim 14$ kpc. It was found that systematic uncertainties in the level of I_b up to $\sim 25\%$ cause comparable uncertainties in the emissivities for $R < 15$ kpc, but have no significant impact on the emissivities for $R > 15$ kpc. This can be understood given the relatively narrow latitude extent of the H I column-densities outside 15 kpc compared to the wider

distribution of the column-densities inside 15 kpc, which more closely resembles the flat background (see Fig. 2).

The emissivity values derived from the SAS-2 data are fully consistent with the COS-B results for the same distance intervals, after correction for the different energy ranges selected. The low-energy result from the SAS-2 data does not provide significantly more information on the gamma-ray spectrum below the COS-B limit of 70 MeV, because the major part of measured gamma-ray events assigned in the SAS-2 analysis to the 35–100 MeV energy range is effectively selected from the same true energy interval as in the case of COS-B for the 70 MeV–150 MeV range (compare Fig. 1 of Lebrun and Paul, 1983, with Fig. 2 of Lebrun et al., 1982). Therefore in the following sections only COS-B data are used.

d) Systematic uncertainties

The radial distribution of the gamma-ray emissivity for the various energy ranges, determined in Sect. IIb and IIc, depends only weakly on the rotation curve used. The use of a somewhat different rotation curve would have changed basically only the absolute distance scale of the radial gas distribution and thus of the radial distribution of the gamma-ray emissivities found. For example, the effect of using a flat rotation curve, rather than the rising curve we have adopted, would simply lower the distance scale in Fig. 5 by about 17% at distances larger than ~ 14 kpc. It would have strengthened the gradient in the low-energy gamma-ray emissivity, while the situation for high energies would have remained unchanged. Therefore, the conclusions drawn in this paper would not have changed.

In principle, the gamma-ray emissivities found should be corrected for a contribution from inverse Compton gamma rays and the small contribution from cosmic-ray interactions with molecular gas. Kniffen and Fichtel (1981) and Sacher and Schönfelder (1983) have shown that although the inverse Compton effect may be significant in the inner Galaxy, it is small ($< 10\%$) for $R > R_{\odot}$ compared to the contribution from the cosmic-ray-matter interactions. For the contribution of gamma rays originating from H_2 , a 3σ upperlimit of $\sim 7\%$ has been determined in Paper I. Inclusion of these effects will negligibly change the emissivities found, because the low-energy photon field and the H_2 gas would have to be spatially well correlated with the HI in the various distance intervals. Since the correlations are probably fairly poor, we expect that the net contribution of these effects is small and split up over the emissivities obtained for the various distance intervals and the derived background level. Thus the emissivity values in Fig. 5 might be too high by a few percent. However, part of these contributions will only have reduced the goodness of the fit, reflected by the statistical uncertainties given. In summary, this means that the emissivity gradients found for the different energy intervals are barely affected.

If the low-energy photon field and the H_2 gas are spatially closely correlated with the HI in the various distance intervals (although unlikely, as mentioned above), it is necessary to estimate their radial distribution to judge their contribution in each interval. From the work of Kniffen and Fichtel (1981), using far-infrared results of Boissé et al. (1981) and the visible-starlight model of Bahcall and Soneira (1980), it can be seen that the density of the low-energy photon field decreases with increasing galacto-centric radius, such that in the plane at $R \cong 15$ kpc the density is about 20% of the local value. Also the amount of H_2 is most probably extremely small at large distances [only a few percent of the clouds listed in the catalogue of Blitz et al. (1982) are located outside

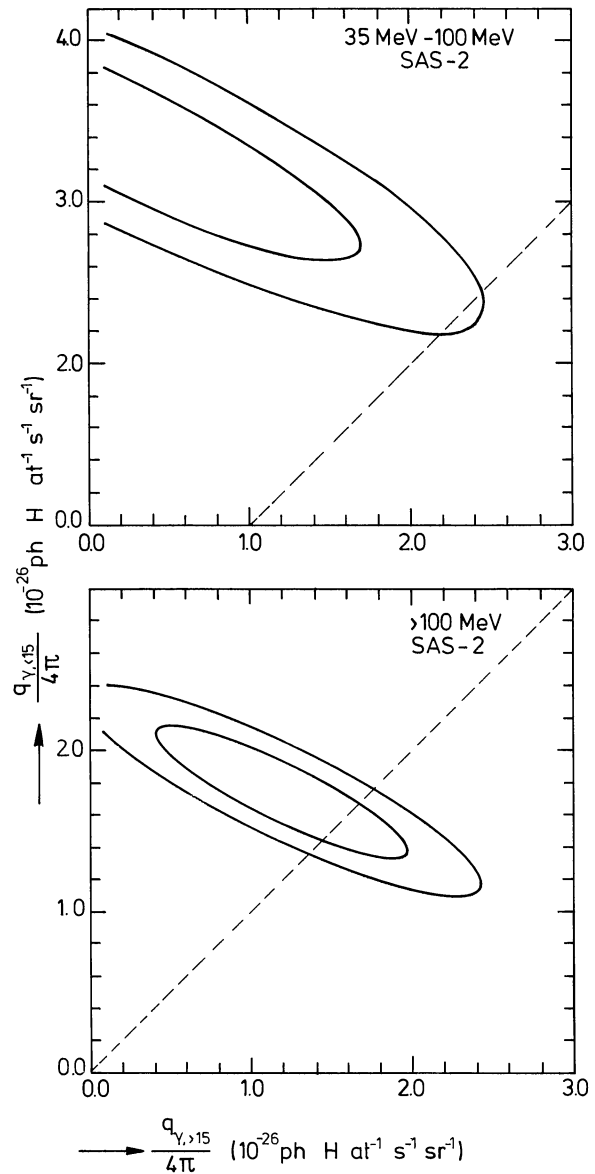


Fig. 6. Likelihood contours of $q_{\gamma, <15}$ and $q_{\gamma, >15}$ for two energy ranges using SAS-2 data. The dashed lines indicate $q_{\gamma, <15} = q_{\gamma, >15}$. See Fig. 4 for a definition of the confidence levels

15 kpc]. Therefore, the major part of the small contribution from inverse Compton gamma-rays and from cosmic-ray interactions with molecular gas, originates at fairly close distances ($R \lesssim 15$ kpc). Only if the low-energy photon field and the H_2 are spatially correlated with the HI, the gamma-ray emissivities within a few kpc outside the solar circle are overestimated in the present analysis. In the worst case (the unlikely case of a perfect spatial correlation), the emissivities found for $R \lesssim 15$ kpc should be lowered by $\sim 20\%$.

III. The gamma-ray spectrum as a function of galacto-centric radius

The analysis described in Sect. II permits the determination of the spectrum of the gamma-ray emissivity in the outer Galaxy at

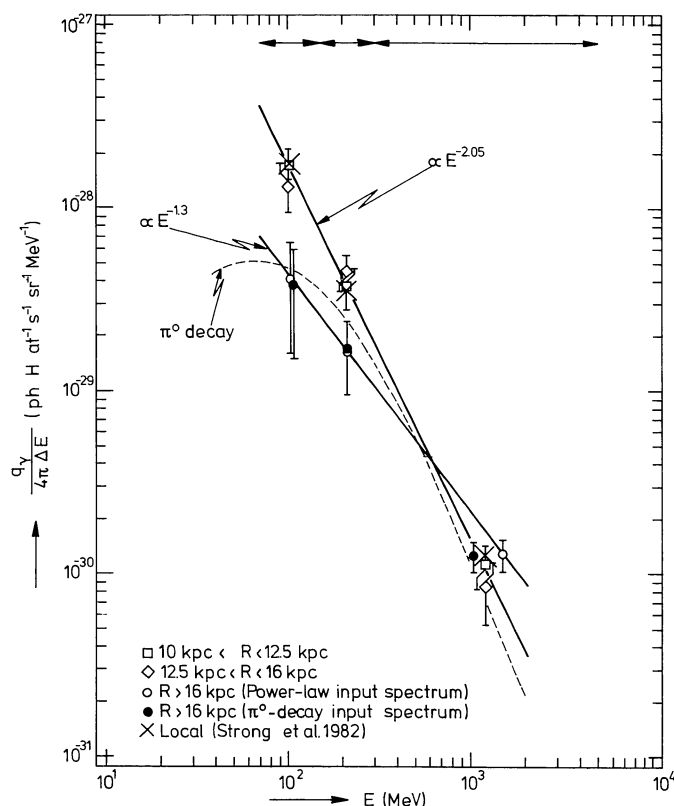


Fig. 7. The gamma-ray emissivity spectrum for $10 \text{ kpc} < R < 12.5 \text{ kpc}$, $12.5 \text{ kpc} < R < 16 \text{ kpc}$ and $R > 16 \text{ kpc}$ determined from COS-B data. The energy ranges in which the emissivities are derived, are indicated at the top of the figure. Formal errors (1σ) are given. For $R > 16 \text{ kpc}$, the effective energies for these ranges and the instrument response are determined using both the best power-law fit and a π^0 -decay spectrum. The solid lines indicate the power-law fits for $R < 12.5 \text{ kpc}$ and $R > 16 \text{ kpc}$. The dashed curve shows the π^0 -decay spectrum of Stephens and Badwahr (1981) (lowered by 10% to fit better the data points) determined from the demodulated proton spectrum given by Burger and Swanenburg (1971)

various distances from the galactic centre. Using the data in Fig. 5, Fig. 7 presents the resulting gamma-ray spectra for $10 \text{ kpc} < R < 12.5 \text{ kpc}$, for $12.5 \text{ kpc} < R < 16 \text{ kpc}$ and for $R > 16 \text{ kpc}$. There is a significant difference between the two spectra for $R < 16 \text{ kpc}$ and the spectrum for $R > 16 \text{ kpc}$, indicating a clear hardening of the gamma-ray spectrum for increasing galacto-centric distances outside the solar circle.

The spectrum for $R < 12.5 \text{ kpc}$ can be fitted by an $E^{-2.05 \pm 0.2}$ power law, in agreement with the local ($\lesssim 1 \text{ kpc}$) spectrum

determined by e.g. Lebrun et al. (1982) and Strong et al. (1982). This is consistent with the assumption made in calculating the instrument response (Sect. IIa). The spectrum for $12.5 \text{ kpc} < R < 16 \text{ kpc}$ is not significantly different from the spectrum for $R < 12.5 \text{ kpc}$.

For $R > 16 \text{ kpc}$, it is evident from the figure that the low-energy component is strongly reduced. Since this is inconsistent with the assumption of an E^{-2} input spectrum made in calculating the instrument response (Sect. IIa), the spectrum for $R > 16 \text{ kpc}$ shown in Fig. 7 was iteratively corrected to account for the harder input spectrum. The spectrum can be fitted equally well by a power-law spectrum with exponent 1.3 ± 0.3 as by a π^0 -decay spectrum in the energy range $70 \text{ MeV} - 5 \text{ GeV}$. Thus Fig. 7 shows that the diffuse gamma-ray spectrum for $R > 16 \text{ kpc}$ is significantly different from the local gamma-ray spectrum and consistent with the π^0 -decay spectrum having the intensity expected from the demodulated local cosmic-ray nuclei spectrum.

Table 2 lists the final gamma-ray emissivities for the three distance intervals shown in Figs 5 and 7. An E^{-2} input spectrum was used in calculating the instrument response for $R < 16 \text{ kpc}$ and a π^0 -decay spectrum for $R > 16 \text{ kpc}$, consistent with the results obtained in this section.

IV. The radial distribution of cosmic-ray electrons and nuclei

Under the assumption that the interactions of cosmic-ray electrons (via bremsstrahlung) and nuclei (via π^0 -decay) with the interstellar gas are responsible for the observed gamma-ray emission (see Sect. II d), knowledge of the radial distribution of gamma-ray emissivities enables the determination of the radial distribution of cosmic rays in the Milky Way. In addition, the energy dependence can be used to study separately the distribution of cosmic-ray electrons and protons.

The overall (power-law) shape of the local gamma-ray emissivity spectrum indicates that the dominant contribution to the low-energy component is due to electron bremsstrahlung. Also, Stephens and Badwahr (1981), starting from the work of Stecker (1973), predicted for π^0 -decay from the demodulated spectrum of cosmic-ray nuclei a gamma-ray emissivity in the $70 \text{ MeV} - 150 \text{ MeV}$ range of $0.44 \cdot 10^{-26} \text{ ph H at}^{-1} \text{ s}^{-1} \text{ sterad}^{-1}$, which is $\sim 30\%$ of the emissivity estimated from the observed local gamma rays (see e.g. Strong et al., 1982). For the $70 \text{ MeV} - 150 \text{ MeV}$ range, about 80% of the bremsstrahlung contribution is due to electrons with $E \lesssim 300 \text{ MeV}$. We have shown in Sect. III that the low-energy gamma-ray component falls off rapidly with R , which implies that there is an evident galacto-centric gradient in the cosmic-ray electron density for electrons with $E \lesssim 300 \text{ MeV}$, as has been known for some years. For the

Table 2. Gamma-ray emissivities for three galacto-centric distance ranges in the second and third galactic quadrants ($|b| < 10^\circ$), as determined from the comparison of I_γ with $N(\text{HI})$ in these distance ranges. Formal errors (1σ) are given (see text)

Distance interval (kpc)	$q_\gamma/4\pi$ ($10^{-26} \text{ photon H atom}^{-1} \text{ s}^{-1} \text{ sterad}^{-1}$)		
	70 MeV–150 MeV	150 MeV–300 MeV	300 MeV–5 GeV
$10 < R < 12.5$	1.39 ± 0.25	0.56 ± 0.14	0.53 ± 0.14
$12.5 < R < 16$	1.05 ± 0.29	0.68 ± 0.15	0.40 ± 0.15
$R > 16$	0.30 ± 0.18	0.26 ± 0.11	0.59 ± 0.12

300 MeV–5 GeV range, about 80% of the bremsstrahlung contribution is due to electrons with $E \lesssim 3$ GeV. It is reasonable to suppose that a similar decrease occurs in this higher-energy electron distribution. In fact, the cosmic-ray lifetime falls with increasing energy. Thus the gradient with R could even be somewhat larger for higher electron energies. Since there is no detectable gradient for the high-energy gamma-ray emissivity, interactions due to the nuclear component of cosmic rays must dominate the gamma-ray spectrum at these energies. The absence of a gradient in the emissivities of the high-energy gamma rays therefore implies that the density of cosmic-ray nuclei, with energies of a few GeV (those responsible for the bulk of the π^0 -decay contribution in the 300 MeV–5 GeV gamma-ray energy range), is constant to within our uncertainties out to large galacto-centric distances. This is supported by the close agreement between the measured gamma-ray emissivity for all distance ranges in the 300 MeV–5 GeV range and that predicted by Stephens and Badwahr (1981) for π^0 -decay from the demodulated spectrum of cosmic-ray nuclei ($0.45 \cdot 10^{-26}$ ph H at $^{-1}$ s $^{-1}$ sterad $^{-1}$). Also the shape of the gamma-ray spectrum for $R > 16$ kpc is significantly different from the local gamma-ray spectrum and not inconsistent with a spectrum due entirely to π^0 -decay, as shown in Fig. 7.

If we assume that the electron density decreases linearly with R and that the electron density is effectively zero for $R \cong 18$ kpc (see Fig. 5a), the radial distribution of the cosmic-ray electron density $n_e(R)$ and of the nuclear density $n_n(R)$ in the outer Galaxy is described by

$$\begin{aligned} n_e(R) &= n_{e0} \left(2.25 - 1.25 \frac{R}{R_\odot} \right) & (10 \text{ kpc} < R < 18 \text{ kpc}) \\ n_e(R) &= 0 & (R > 18 \text{ kpc}), \\ n_n(R) &= n_{n0}, & \end{aligned} \quad (2)$$

$$n_n(R) = n_{n0}, \quad (3)$$

where n_{e0} and n_{n0} are the local interstellar electron and nuclear densities respectively.

Li Ti Pei and Wolfendale (1981) concluded from an analysis of a small subset of the COS-B data base that cosmic-ray nuclei do show a strong gradient in the outer Galaxy. However their conclusions were based on simple longitude correlations in a limited region of the sky ($\sim 5\%$ of the region analyzed in the present analysis).

The average gamma-ray spectra in the second and third galactic quadrants are harder than the average spectra in the first and fourth galactic quadrants. (see e.g. Mayer-Hasselwander, 1983). This could be the result of a continuous softening of the gamma-ray emission toward inner-galactic regions, as discussed by Hermsen and Bloemen (1983). Furthermore, Lebrun et al. (1983), from analysis of high-energy gamma-ray, H I and CO distributions in the first quadrant, did not find evidence for a strong gradient of cosmic-ray nuclei.

V. Comparison with synchrotron emission

Low-frequency radio-continuum emission is primarily synchrotron emission resulting from the interaction of cosmic-ray electrons with the interstellar magnetic field. Electrons of energy $\lesssim 300$ MeV, which are responsible for the gamma rays in the low-energy range, emit synchrotron radiation at ~ 30 MHz in the galactic field of 2–3 μ G. Therefore the distribution of electrons

derived in the previous sections can be compared directly with the result based on low-frequency continuum surveys.

Webber et al. (1980) derived the local synchrotron emissivity $\varepsilon_v(R_\odot)$ at 30 MHz from observations toward H II regions, and then used this to derive an effective pathlength $R_{\text{eff}} = 2.1$ kpc towards the anticentre, where

$$R_{\text{eff}} = \left\{ \int_{R_\odot}^{\infty} \varepsilon_v(R) dR \right\} / \varepsilon_v(R_\odot) \quad (4)$$

From the linear law given in Eq. 2, the COS-B gamma-ray data imply an effective pathlength of ~ 4 kpc for the electrons. Hence, on a large scale, the synchrotron and gamma-ray values both show the electron distribution falling off. The difference in the two R_{eff} values is within the uncertainties of the two methods; we note nevertheless that if the magnetic field also falls off we expect $R_{\text{eff, sync}} < R_{\text{eff, electrons}}$, as observed.

Phillipps et al. (1981), modelling the 408 MHz nonthermal emission, showed that, on a large scale, the observed emission is best described by a decreasing synchrotron emissivity as a function of galacto-centric radius. Since their unfolding technique cannot be applied outside the solar circle, they determined the distance out to which the azimuthal and radial variation of the emissivity, deduced from within the solar circle, must be extrapolated in order to match the observed anticentre brightness temperature. For a powerlaw [$\varepsilon(R) \propto R^{-1.9}$] and an exponential [$\varepsilon(R) \propto \exp(-R/3.9 \text{ kpc})$] variation, they found 16 kpc and 20 kpc, respectively, which corresponds to an effective path length of $R_{\text{eff}} = 3.5$ –4 kpc. Hence, if the magnetic field does not show a strong gradient outside the solar circle, also the distribution of the few-GeV electrons, responsible for the 408 MHz nonthermal emission, seems to fall off in a similar manner as the lower-energy electrons.

It can be concluded that the electron-density distribution decreases much more rapidly than the H I surface density as a function of R . One may compare the results for the Milky Way with the H I and radio-continuum emission seen in other spiral galaxies. Typically it is found that the galacto-centric distribution of the H I emission is broader than that of the synchrotron emission (see e.g. van der Kruit and Allen, 1976; Sancisi and Allen, 1979), in qualitative agreement with what is found here for the Galaxy.

VI. Implications for cosmic-ray origin

The results presented above place constraints on the distribution of cosmic-ray sources. The strong decrease of the cosmic-ray electron density in the outer Galaxy clearly confirms its galactic origin. The interpretation of the flat nucleus distribution is beyond the scope of this paper, but a few general observations can be made.

If the sources of both species are similarly distributed in the Galaxy, extensive diffusion of the nuclei into the outer Galaxy is required to reproduce their observed flat distribution. Disk confinement will encounter difficulties in such a model and most probably a large halo would have to be invoked. However, models involving a large halo, with diffusion (Ginzburg and Syrovatskii, 1964; Ginzburg et al., 1980) or diffusion and convection (Owens and Jokipii, 1977) generally produce gradients in the cosmic-ray density on scales 3 kpc in the z -direction, and a similar scale should hold in the radial direction outside the source region. An explicit example of the distribution of cosmic rays in a diffusive halo model

for the Galaxy is given in Strong (1977), and this shows a steep radial gradient. An alternative model involving Galactic origin would be a large homogeneous halo, but this is unlikely on physical grounds.

The data are consistent with an extragalactic origin for the nuclei (Brecher and Burbidge, 1972; Burbidge, 1974) either in its "universal" or "local supercluster" forms. The former is considered unlikely because of the problem of transporting the particles over intercluster distances (Burbidge, 1974). The local supercluster theory avoids these problems, and has also been proposed to explain the distribution of cosmic rays above 10^{18} eV (see e.g. Brecher and Burbidge, 1972; Burbidge, 1974; Strong et al., 1974; Wdowczyk and Wolfendale, 1979; Astley et al., 1981).

VII. Summary and conclusions

Combining the distance information contained in the 21-cm H I data with the gamma-ray data of the COS-B experiment, information is obtained on the radial distribution of gamma rays and cosmic rays in the outer Galaxy. A different behaviour is found for the 70 MeV–150 MeV gamma rays compared to the higher-energy gamma rays, which can be explained by differences between the cosmic-ray electron and nuclei distributions. Namely the gamma-ray emissivity in the energy range 70 MeV–150 MeV exhibits a strong gradient in the outer Galaxy, while the emissivity for energies above 300 MeV remains constant within $\sim 20\%$ and equal to the local value out to large (~ 20 kpc) galacto-centric distances. The low-energy gamma-ray emissivity for $R > 16$ kpc is down by at least 50% compared to the local value. In other words, the measured gamma-ray energy spectrum becomes increasingly harder with increasing R . The gamma-ray spectrum for $10 \text{ kpc} < R < 12.5 \text{ kpc}$ is best fitted by a power-law spectrum with index 2.05 ± 0.2 , consistent with the local (≤ 1 kpc) spectrum. The spectrum for $R > 16$ kpc can be fitted equally well by a power-law spectrum with index 1.3 ± 0.3 as by a π^0 -decay spectrum. These results are interpreted as *i*) a decrease of the density of cosmic-ray electrons with energies up to several hundreds of MeV, such that at large (~ 18 kpc) galacto-centric distance the electron density is approximately zero, and *ii*) a near constancy of the density of cosmic-ray nuclei with energies of a few GeV, out to large distances.

The variation of the electron component is consistent with low-frequency radio-continuum observations. The galactic origin of electrons with energies up to several hundreds of MeV is confirmed, while for cosmic-ray nuclei with energies of a few GeV either confinement in a large halo or an extragalactic origin is suggested by the data.

Acknowledgements. L.B. gratefully acknowledges support from the Netherlands Organization for the Advancement of Pure Research (ZWO), Grant No. 0407/83 from the NATO Scientific Affairs Division, and the General Research Board of the University of Maryland. The authors thank K. Paizis for helpful discussions and the referee A.W. Wolfendale for useful comments.

References

- Arnaud, K., Li Ti Pei, Riley, P.A., Wolfendale, A.W., Dame, T.M., Brock, J.E., Thaddeus, P.: 1982, *Monthly Notices Roy. Astron. Soc.* **201**, 745
- Astley, S.M., Cunningham, G., Lloyd-Evans, J., Reid, R.J.O., Watson, A.A.: 1981, *Proc. 17th Intern. Cosmic Ray Conf.* **2**, 156
- Bahcall, J.N., Soneira, R.M.: 1980, *Astrophys. J. Letters* **238**, L17
- Blitz, L., Fich, M., Stark, A.A.: 1980, in *Interstellar Molecules*, ed. B. Andrew, Reidel Dordrecht, p. 213
- Bloemen, J.B.G.M., Blitz, L., Hermsen, W.: 1984, *Astrophys. J.* (in press)
- Boissé, P., Gispert, R., Coron, N., Wijnbergen, J., Serra, G., Ryter, C., Puget, J.L.: 1981, *Astron. Astrophys.* **94**, 265
- Brecher, K., Burbidge, G.R.: 1972, *Astrophys. J.* **174**, 253
- Burbidge, G.R.: 1974, *Phil. Trans. Roy. Soc. Lond. A* **277**, 481
- Burger, J.J., Swanenburg, B.N.: 1971, *Proc. 12th Intern. Cosmic Ray Conf.* **5**, 1858
- Dodds, D., Strong, A.W., Wolfendale, A.W.: 1975, *Monthly Notices Roy. Astron. Soc.* **171**, 569
- Eadie, W.T., Drijard, D., James, F.E., Roos, M., Sadoulet, B.: 1971, *Statistical Methods in Experimental Physics*, North-Holland, Amsterdam, p. 230
- Fichtel, C.E., Hartman, R.C., Kniffen, D.A., Thompson, D.J., Ögelman, H.B., Tümer, T., Özel, M.E.: 1978, *NASA Technical Memorandum 79650*
- Ginzburg, V.L., Syrovatskii, S.I.: 1964, *The origin of cosmic rays*, Pergamon Press, Oxford
- Ginzburg, V.L., Khazan, Y.M., and Ptuskin, V.S.: 1980, *Astrophys. Space Sci.* **68**, 295
- Heiles, C., Habing, H.J.: 1974, *Astron. Astrophys. Suppl.* **14**, 1
- Henderson, A.P., Jackson, P.D., Kerr, F.J.: 1982, *Astrophys. J.* **263**, 116
- Hermsen, W.: 1980, Ph. D. Thesis, University of Leiden, The Netherlands
- Hermsen, W., Bloemen, J.B.G.M.: 1983, in *Surveys of the Southern Galaxy*, eds. W. B. Burton, F. P. Israel, Reidel, Dordrecht, p. 65
- Issa, M.R., Riley, P.A., Strong, A.W., Wolfendale, A.W.: 1980, *Nature* **287**, 810
- Issa, M.R., Riley, P.A., Strong, A.W., Wolfendale, A.W.: 1981, *J. Phys. G7*, 973
- Kniffen, D.A., Fichtel, C.E.: 1981, *Astrophys. J.* **250**, 389
- van der Kruit, P.C., Allen, R.J.: 1976, *Ann. Review of Astron. Astrophys.* **14**, 417
- Kulkarni, S.R., Blitz, L., Heiles, C.: 1982, *Astrophys. J. Letters* **259**, L63
- Lebrun, F., Bignami, G.F., Buccheri, R., Caraveo, P.A., Hermsen, W., Kanbach, G., Mayer-Hasselwander, H.A., Paul, J.A., Strong, A.W., Wills, R.D.: 1982, *Astron. Astrophys.* **107**, 390
- Lebrun, F., Paul, J.A.: 1983, *Astrophys. J.* **266**, 276
- Lebrun, F., Bennett, K., Bignami, G.F., Bloemen, J.B.G.M., Buccheri, R., Caraveo, P.A., Gottwald, M., Hermsen, W., Kanbach, G., Mayer-Hasselwander, H.A., Montmerle, T., Paul, J.A., Sacco, B., Strong, A.W., Wills, R.D., Dame, T.M., Cohen, R.S., Thaddeus, P.: 1983, *Astrophys. J.* **274**, 23
- Li Ti Pei, Wolfendale, A.W.: 1981, *J. Phys. G7*, L157
- Mayer-Hasselwander, H.A., Bennett, K., Bignami, G.F., Buccheri, R., Caraveo, P.A., Hermsen, W., Kanbach, G., Lebrun, F., Lichti, G.G., Masnou, J.L., Paul, J.A., Pinkau, K., Sacco, B., Scarsi, L., Swanenburg, B.N., Wills, R.D.: 1982, *Astron. Astrophys.* **105**, 164
- Mayer-Hasselwander, H.A.: 1983, in *Kinematics, Dynamics and Structure of the Milky Way*, ed. W.L.H. Shuter, Reidel, Dordrecht, p. 223
- Owens, A.J., Jokipii, J.R.: 1977, *Astrophys. J.* **215**, 677
- Phillipps, S., Kearsy, S., Osborne, J.L., Haslam, C.G.T., Stoffel, H.: 1981, *Astron. Astrophys.* **98**, 286
- Sacher, W., Schönfelder, V.: 1983, *Space Sci. Rev.* **36**, 249

- Sancisi, R., Allen, R.J.: 1979, *Astron. Astrophys.* **74**, 73
- Stecker, F.W.: 1971, *Cosmic Gamma Rays*, Mono Book Corp., Baltimore
- Stecker, F.W.: 1973, *Astrophys. J.* **185**, 499
- Stephens, S.A., Badwahr, G.D.: 1981, *Astrophys. Space Sci.* **76**, 213
- Strong, A.W., Wdowczyk, J., Wolfendale, A.W.: 1974, *J. Phys. A* **7**, 1767
- Strong, A.W.: 1977, *Monthly Notices Roy. Astron. Soc.* **181**, 311
- Strong, A.W., Wolfendale, A.W.: 1981, *Phil. Trans. R. Soc. Lond. A* **301**, 541
- Strong, A.W., Lebrun, F.: 1982, *Astron. Astrophys.* **105**, 159
- Strong, A.W., Bignami, G.F., Bloemen, J.B.G.M., Buccheri, R., Caraveo, P.A., Hermsen, W., Kanbach, G., Lebrun, F., Mayer-Hasselwander, H.A., Paul, J.A., Wills, R.D.: 1982, *Astron. Astrophys.* **115**, 404
- Strong, A.W., Bennett, K., Bignami, G.F., Bloemen, J.B.G.M., Buccheri, R., Caraveo, P.A., Hermsen, W., Lebrun, F., Mayer-Hasselwander, H.A., Özel, M.E.: 1984 (in preparation)
- Swanenburg, B.N., Bennett, K., Bignami, G.F., Buccheri, R., Caraveo, P.A., Hermsen, W., Kanbach, G., Lichti, G.G., Masnou, J.L., Mayer-Hasselwander, H.A., Paul, J.A., Sacco, B., Scarsi, L., Wills, R.D.: 1981, *Astrophys. J. Letters* **243**, L69
- Thompson, D.J., Fichtel, C.E.: 1982, *Astron. Astrophys.* **109**, 352
- Wdowczyk, J., Wolfendale, A.W.: 1979, *Proc. 16th Intern. Cosmic Ray Conf.* **2**, 154
- Weaver, H., Williams, D.R.W.: 1973, *Astron. Astrophys. Suppl.* **8**, 1
- Webber, W.R., Simpson, G.A., Cane, H.V.: 1980, *Astrophys. J.* **236**, 448
- Williams, D.R.W.: 1973, *Astron. Astrophys. Suppl.* **8**, 505
- Wolfendale, A.W.: 1981, in *Origin of cosmic rays*, Reidel, Dordrecht, p. 309